Received: 31 January 2022 | Revised: 22 March 2022 | Accepted: 18 April 2022

DOI: 10.1111/jnc.15617

Journal of Neurochemistry JNC The Official Journal of the International Society for Neurochemistry WILEY

ORIGINAL ARTICLE

Selective activation and down-regulation of Trk receptors by neurotrophins in human neurons co-expressing TrkB and TrkC

Sarah Ateaque[1] | Spyros Merkouris[1] | Sean Wyatt[1] | Nicholas D. Allen[1] | Jia Xie[2] | Peter S. DiStefano[3] | Ronald M. Lindsay[3] | Yves-Alain Barde[1]

[1]School of Biosciences, Cardiff University, Cardiff, Wales, UK

[2]The Scripps Research Institute, La Jolla, California, USA

[3]Zebra Biologics, Concord, Massachusetts, USA

Correspondence
Yves-Alain Barde, School of Biosciences, Cardiff University, Cardiff CF10 3AX, Wales, UK.
Email: bardey@cardiff.ac.uk

Present address
Spyros Merkouris, VIB Center for Brain & Disease Research, Leuven

Jia Xie, Sanofi Institute for Biomedical Research, Jiangsu, China

Funding information
The Neuroscience and Mental Health Research Institute; The Sêr Cymru progamme of the Welsh Government; Zebra Biologics

Cover Image for this issue: https://doi.org/10.1111/jnc.15406

Abstract

In the central nervous system, most neurons co-express TrkB and TrkC, the tyrosine kinase receptors for brain-derived neurotrophic factor (BDNF) and neurotrophin-3 (NT3). As NT3 can also activate TrkB, it has been difficult to understand how NT3 and TrkC can exert unique roles in the assembly of neuronal circuits. Using neurons differentiated from human embryonic stem cells expressing both TrkB and TrkC, we compared Trk activation by BDNF and NT3. To avoid the complications resulting from TrkB activation by NT3, we also generated neurons from stem cells engineered to lack TrkB. We found that NT3 activates TrkC at concentrations lower than those of BDNF needed to activate TrkB. Downstream of Trk activation, the changes in gene expression caused by TrkC activation were found to be similar to those resulting from TrkB activation by BDNF, including a number of genes involved in synaptic plasticity. At high NT3 concentrations, receptor selectivity was lost as a result of TrkB activation. In addition, TrkC was down-regulated, as was also the case with TrkB at high BDNF concentrations. By contrast, receptor selectivity as well as reactivation were preserved when neurons were exposed to low neurotrophin concentrations. These results indicate that the selectivity of NT3/TrkC signalling can be explained by the ability of NT3 to activate TrkC at concentrations lower than those needed to activate TrkB. They also suggest that in a therapeutic perspective, the dosage of Trk receptor agonists will need to be taken into account if prolonged receptor activation is to be achieved.

KEYWORDS
arc/Arg3.1, BDNF, Neurotrophins, receptors, RNAseq, synaptic plasticity

1 | INTRODUCTION

The physiology of neurotrophins, including their selectivity, is best understood in the peripheral nervous system (PNS) where their limited availability regulates the number of surviving neurons in developing ganglia (Davies 1994; Huang & Reichardt, 2001). In line with this well-established notion, the loss of one neurotrophin allele accentuates normally occurring cell death in these ganglia

Abbreviations: BDNF, brain-derived neurotrophic factor; CNS, central nervous system; hESCs, human embryonic stem cells; NT3, neurotrophin-3; *NTRK2*, human gene encoding TrkB; *NTRK3*, human gene encoding TrkC; PNS, peripheral nervous system; P-Trk, tyrosine phosphorylated Trk receptor; RNAseq, RNA sequencing TrkC; RT-qPCR, real-time quantitative polymerase chain reaction.

(Erickson et al., 1996) whilst conversely, increasing neurotrophin levels reduces naturally occurring cell death (Hamburger et al., 1981; Hofer & Barde, 1988). In the developing central nervous system (CNS) where the effects of neurotrophins on neuronal survival are much less apparent compared to peripheral neurons (Rauskolb et al., 2010), the significance of gene dosage has also been noted, for example on neurotransmission. In particular, the loss of just one *Bdnf* allele severely impacts long-term potentiation in CA1 induced by high-frequency stimulation of the Schaffer collaterals (Korte et al., 1995; Patterson et al., 1996). Hitherto, the bulk of biochemical studies on neurotrophin signalling involving CNS neurons have been performed with BDNF at saturating concentrations and led to the conclusion that exposing neurons to nM concentrations of BDNF causes a prolonged down-regulation of TrkB (Arevalo et al., 2006; Frank et al., 1996; Frank et al., 1997; Knusel et al., 1997; Sommerfeld et al., 2000). While the overwhelming majority of studies on the role of neurotrophins in the CNS have focused on BDNF and TrkB (Wang et al., 2022), brain-wide RNAseq experiments in both mouse and human tissue indicate that most neurons co-express the TrkB and TrkC receptors (see Figure S1). In addition, both receptors play a role during the development of the mouse cortex (Puehringer et al., 2013). These features have complicated the understanding of NT3-mediated signalling as NT3 has long been known to activate TrkB and TrkC at similar concentrations, with EC_{50} of about 1 nM in heterologous expression systems (Barbacid, 1994). By contrast, detailed binding studies with PNS neurons have reported affinities in the pM range (Rodriguez-Tebar et al., 1991). As the few studies on the role of NT3/TrkC signalling during mouse brain development do indicate unique as well as essential roles for both components in circuit assembly (Joo et al., 2014), we set out to explore NT3-mediated TrkC signalling using neurons derived from hESCs. These neurons were found to express both TrkB and TrkC, at ratios similar to those found in the human and mouse brains. As the antibodies used to monitor Trk activation do not distinguish between activated TrkB and TrkC, we also engineered hESCs to eliminate TrkB activation by BDNF and other ligands. Gene expression changes downstream of TrkC activation by NT3 were monitored by RNAseq using these mutant neurons.

2 | MATERIALS AND METHODS

2.1 | hES cell culture and neuronal differentiation

The human embryonic stem cell line hESCs H9, WAe009-A (Thomson et al., 1998) and isogenic *NTRK2* targeted or non-targeted clones C9, B1, D2 and A10 were grown on matrigel-coated plates (Corning, catalogue number: 534230) and in mTeSR medium (STEMCELL Technologies, catalogue number: 85857) and hESCs were passaged using ReLeSR (STEMCELL Technologies, catalogue number: 05872) according to the manufacturer's instructions. As previously described for mouse ESCs (Bibel et al., 2004; Bibel et al., 2007), hES cells were repeatedly plated and re-plated at very low density to ensure the selection of most rapidly dividing cells, a procedure selecting against cells that have begun to differentiate (Ying et al., 2008) and aneuploid cells (Hwang et al., 2021). Neural differentiation was performed as previously described (Merkouris et al., 2018). Briefly, hESCs were grown to confluency, washed 3 times with phosphate-buffered saline (PBS, Invitrogen Life Technologies, catalogue number: 10010023) and fed daily with neural induction medium containing Advanced DMEM:F12 (with Glutamax); 1% penicillin/streptomycin (all from Life Technologies, catalogue numbers: 12634028, 35050061, 15070063); 10 μM SB431542 (Abcam, catalogue number: ab120163) 1 μM LDN 193189 (Tocris Bioscience, catalogue number: 6053); 1.5 μM IWR1 (Tocris Bioscience, catalogue number: 3532) and 2% NeuroBrew-21 without retinoic acid (Miltenyi Biotec, catalogue number: 130097263). At day 8, neural progenitors were dissociated with Accutase (Life Technologies, catalogue number: 00455556) and re-seeded in an expansion medium containing Advanced DMEM-F12 supplemented with 2% NeuroBrew-21 without retinoic acid (Miltenyi Biotec), 0.2 μM LDN193189, 1.5 μM IWR1 and 25 ng/mL Activin A (Peprotech, catalogue number 12014). Neuronal differentiation and maturation were performed as previously described (Telezhkin et al., 2016). Neural progenitors were seeded on poly-D-lysine (ThermoFisher Scientific, catalogue number: A3890401) and growth factor-reduced matrigel-coated surfaces at a density of 1 million cells per well of 12-well plates or 150000 cells per 13 mm coverslip and cultured for 7 days in SCM1 medium containing Advanced DMEM F12 (with Glutamax), 1% penicillin/streptomycin, 2% NeuroBrew21 with retinoic acid (Miltenyi Biotec, catalogue number: 130093566), 2 μM PD0332991 (Tocris Bioscience, catalogue number: 4786), 10 μM DAPT (Tocris Bioscience, catalogue number: 2634), 0.6 mM CaCl2 to give 1.8 mM CaCl2 in final complete medium (Sigma-Aldrich, catalogue number: 499609), 3 μM CHIR 99021 (Tocris Bioscience, catalogue number: 4953), 10 μM Forskolin (Tocris Bioscience, catalogue number: 199), 300 μM GABA (Tocris Bioscience, catalogue number: 0344) and 200 mM ascorbic acid (Sigma- Aldrich, catalogue number: A4544). The medium was replaced at day 7 post-plating by SCM2 medium which contained equal parts Advanced DMEM/F12 with Glutamax and Neurobasal A (ThermoFisher Scientific, catalogue number: 21103049), 1% penicillin/streptomycin, 2% NeuroBrew-21 with retinoic acid, 2 μM PD0332991, 3 μM CHIR 99021, 0.3 mM CaCl2 (1.8 mM CaCl2 final), and 200 μM ascorbic acid. Plated progenitors and the resulting neurons were maintained for up to day 35 before experimentation and all experiments were carried out between days 27 and 33. All western blot results were reproduced a minimum of three times with three independent differentiations. Cultures were regularly checked for mycoplasma contamination using the LookOut Mycoplasma PCR Detection kit (Sigma-Aldrich, catalogue number: MP0035) according to the manufacturer's instructions. Recombinant NT3 and BDNF were produced in *E. coli* and provided by Amgen/Regeneron partners. The concentrations indicated refer to neurotrophin dimers.

2.2 | CRISPR targeting

NTRK2 mutant H9 hESC clones were generated by CRISPR gene editing. Guide RNAs targeting exon 5 of *NTRK2* were selected using Deskgen CRISPR design tools (www.deskgen.com). CRISPR was performed using ribonucleoprotein technology (RNP) (Bruntraeger et al., 2019). Briefly, 2 nM of each guide RNA (TCGTCCTGGATAAGGTGGCATGG, GTCGCTGCACCAGATCCGAGAGG,ACACTGTTAGGCTCCAATCT CGG) and 20 nmol ATTO™ 550 labelled Alt-R® CRISPR-Cas9 tracrRNA were complexed in IDT buffer. The RNP complexes were formed immediately prior to use by mixing the crRNA:tracrRNA complexes with Alt-R® S.p. HiFi Cas9 Nuclease V3 (all CRISPR reagents were purchased from Integrated DNA Technologies). RNP complexes were delivered to H9 hESCs by Amaxa nucleofection. Briefly, H9 ESCs pre-treated for 1 h with 10 μM Y-27632 (Tocris Bioscience, catalogue number: 1254) were dissociated into single-cell suspension using Accutase. 1×10^6 cells were resuspended in Amaxa P3 nucleofection buffer (Lonza, catalogue number: V4XP3032), mixed with Cas9 RNP complex and nucleofected using programme CA137 on the Amaxa-4D nucleofector. After overnight culture in mTesR medium containing 10 μM Y-27632, nucleofected cells were sorted by flow cytometry (BD FACS Aria Fusion) and the brightest Atto550 labelled cells (~5000 cells) were re-plated at clonal density onto Matrigel-coated 10 cm plates. Cells were fed with mTesR medium containing 10 μM Y-27632 and 1% penicillin/streptomycin for the first 3 days followed by mTesR only thereafter. Colonies derived from single cells were manually picked on day 7 into 96-well plates and the plates were replica-plated by passaging with ReLeSR, allowing one plate to be used for DNA analysis. Clone genotyping was carried out using DNA extracted from each well of the 96 well plate using QuickExtract DNA Extraction Solution (Lucigen, catalogue number: QE09050) according to the manufacturer's instructions. Samples were genotyped using PCR primers (forward: 5′-CCCTGTAAAGCGGTTCGCTA-3′ and reverse: 5′-CCCACTCTTGGGACAGCATT-3′) designed to flank the CRISPR-targeted region and PCR products for wild type and mutant alleles were analysed by 2% agarose gel electrophoresis. PCR amplicons from candidate-edited clones were gel extracted (Qiagen, catalogue number: 28706X4) for Sanger sequencing (Eurofins) and sequences analysed using CRISPR-ID software (http://crispid.gbiomed.kuleuven.be/).

2.3 | RNA extraction

Total RNA was extracted from human neurons using the RNeasy Mini kit (Qiagen, catalogue number: 74104). Cultures were washed with D-PBS (ThermoFisher Scientific, catalogue number: 1404017) and lysed with 350 μl of RLT RNA lysis buffer (Qiagen, catalogue number: 79216) containing 1% β-2-mercaptoethanol (Sigma-Aldrich, catalogue number: M6250). Lysates were either frozen at −80 °C or processed with the RNeasy Mini Kit according to the manufacturer's instructions, including a DNase treatment for 15 min at room temperature (22°C) (Qiagen, catalogue number: 79254).

2.4 | RT-qPCR

The levels of full-length, kinase domain-positive *NTRK2 and NTRK3* mRNAs were quantified by RT-qPCR relative to a geometric mean of mRNAs for *GAPDH*, *TBP*, *GAD2* and *GAD1* (Vandesompele et al., 2002). Total RNA was extracted from dissected tissues with the RNeasy Mini extraction kit (Qiagen). A 500 ng H9 total RNA was reverse transcribed, for 1 h at 45°C, using AffinityScript (Agilent) in a 25 μl reaction according to the manufacturer's instructions. A 2 μl of cDNA was amplified in a 20 μl reaction volume using Brilliant III ultrafast qPCR master mix reagents (Agilent Technologies). PCR products were detected using dual-labelled (FAM/BHQ1) hybridization probes specific to each of the cDNAs (Eurofins). *NTRK2* and *NTRK3* primers and probes were directed against full-length, kinase domain encoding transcripts. The PCR primers were: *NTRK2* forward: 5′-TTC CCA TCA CCA GAA ATG-3′ and reverse: 5′-GCT TGA GAA ACA AAC CAG-3′; *NTRK3* forward: 5′-TCT GCT AGT GAA GAT TGG-3 ′ and reverse: 5′-TCC CAC CCT GTA ATA ATC-3′; *GAD2* forward: 5′-CCA GAA GTC AAG GAG AAA-3′ and reverse: 5′-GTC TGT TCC AAT CCC TAA-3′; *GAD1* forward: 5′-CAG AGA AGA ATT TGA GAT GG-3′ and reverse: 5′-GGC TTT GTG GAA TAT ACC-3′; *GAPDH* forward: 5′-TGG TCT CCT CTG ACT TCA-3′ and reverse: 5′-GCT GTA GCC AAA TTC GTT G-3′; *TBP* forward: 5′-CTC ACA GAC TCT CAC AAC-3′ and reverse: 5′-AGG TCA AGT TTA CAA CCA A-3′. Dual-labelled probes were: *NTRK2*: 5′-FAM-CTA TCA TCA CAA CCT ACG AAG ACA AA-BHQ1-3′; *NTRK3*: 5′-FAM-ATG TCC AGA GAT GTC TAC AGC-BHQ1-3′; *GAD2*: 5′-FAM-TGC TCT TCC CAG GCT CAT TGC-BHQ1-3; *GAD1*: 5′-FAM-CAA TGG CGA GCC TGA GCA CA-BHQ1-3′; *GAPDH*: 5′-FAM-AGC GAC ACC CAC TCC TCC AC-BHQ1-3′ and *TBP*: 5′-FAM-CGG GCA CCA CTC CAC TGT ATC C -BHQ1-3′. Forward and reverse primers were used at a concentration of 250 nM and dual-labelled probes were used at a concentration of 500 nM. PCR was performed using the Mx3000P platform (Agilent) using the following conditions: 95°C for 3 min followed by 45 cycles of 95°C for 10 s and 60°C for 35 seconds. Reverse transcribed *NTRK2*, *NTRK3*, *GAD2*, *GAD1*, *GAPDH* and *TBP* cDNAs were quantified by reference to standard curves comprising serial fivefold dilutions of cDNAs encoding *NTRK2*, *NTRK3*, *GAD65*, *GAD67*, *GAPDH* and *TBP*. Standard curves were run for each primer/probe combination. Primer and probe sequences were designed using Beacon Designer software (Premier Biosoft).

2.5 | RNAseq analysis

A10 neurons were treated for 2 and 24 h with NT3 (2 nM), RNA was extracted and integrity assessed on an Agilent RNA 6000 Pico chip using the Agilent 2100 Bioanalyzer (Agilent Technologies). RNA (500 ng) was used to produce the cDNA library with the Tru-Seq protocol (Illumina) and sequenced with an Illumina HiSeq 4000 system. RNAseq single-end fastq files were mapped to human assembly genome GRCh38 using the STAR package. Transcript counts were produced with FeatureCounts, and data were normalised using the

Bioconductor package. Gene expression values and differentially expressed genes were obtained using DeSeq2 package in fragments per kilobase of transcript per million mapped reads (FPKM). Principal component analysis (CA) was used to analyse how different samples relate to each other based on overall expression profiles. Software used for RNAseq data processing and analysis was: Trimgalore (version 0.6.4), FastQC (version 0.11.8), MultiQC (version 1.7), STAR package (version 2.7.3a), Picard (version 2.20.2), samtools (version 1.9), bamtools (version 2.5.1), featureCountsubread/2.0.0-binary, R (version 4.0.3) and Python (version 3.6.4).

2.6 | Accession numbers

Full RNAseq data are available in the ArrayExpress database (http://www.ebi.c.uk/arrayexpress) under accession number E-MTAB-11566.

2.7 | Cell lysis and protein extraction

Neurons were plated on 12-well plates and incubated with the appropriate ligand. Prior to lysis, the cultures were washed with PBS, and subsequently lysed with 70 µl of RIPA lysis buffer: 50 mM Tris–HCl (Sigma-Aldrich, catalogue number: T6066, pH 7.4), 150 mM NaCl (Sigma-Aldrich, catalogue number: S9888), 1 mM EDTA (Sigma-Aldrich, catalogue number: ED), 1% Triton-X-100 (Sigma-Aldrich, catalogue number: T9284), 0.2% sodium deoxycholate (Sigma-Aldrich, catalogue number: D6750), 0.1% SDS (Sigma-Aldrich, catalogue number: L3771) and supplemented with protease and phosphatase inhibitor cocktail mix (Sigma-Aldrich, catalogue numbers: P8340, P2850) at 1:100 dilution, 100 mM 1,10-Phenanthroline (Sigma-Aldrich, catalogue number: P9375), 100 mM 6-aminohexanoic acid (Sigma-Aldrich, catalogue number: 07260), 10 mg/ml aprotinin (Sigma-Aldrich, catalogue number: ROAPRO) and 2 mM sodium orthovanadate (Sigma-Aldrich, catalogue number: S6508). Cell lysates were kept on ice for 10 min, then centrifuged for 15 min at 21 130 g and the supernatant was transferred to a new tube prior to western blot analysis, or storage at −80°C.

2.8 | Western blotting

Protein was separated on 15-well 4–12% NUPAGE gradient gels (ThermoFisher Scientific, catalogue number: NP0323) and transferred to nitrocellulose membranes using the wet transfer Mini-Trans Blot Cell (BIO-RAD, catalogue number: 1703930). The blots were probed with rabbit monoclonal anti-Pan-Trk (Abcam, mAB, catalogue number: ab76291), rabbit monoclonal anti-P-Trk (Cell Signalling, mAb, catalogue number: 4621) diluted 1:4000, goat polyclonal anti-TrkB (R&D Systems, pAB, catalogue number: AF1494) diluted 1:2000, goat polyclonal anti-TrkC (R&D Systems, pAB, catalogue number: AF373) diluted 1:2000. Both anti-TrkB and anti-TrkC antibodies were validated using lysates of CHO cells over-expressing human TrkB and human TrkC, respectively. Mouse monoclonal anti-Arc (Santa Cruz, mAB, catalogue number: sc-17839) diluted 1:100 or mouse monoclonal anti-synaptophysin (Sigma-Aldrich, mAB, catalogue number: S5768) diluted 1:2000. Primary antibodies were detected with donkey anti-Rabbit HRP-conjugated (Promega, catalogue number: W4011), anti-goat HRP-conjugated (Santa-Cruz, catalogue number: sc-2354) and anti-Mouse HRP-conjugated secondary (Promega, catalogue number: W4021) antibodies diluted 1:2000 followed by developing, using the WesternBright ECL Kit (Advansta, catalogue number: K12045). Blots were visualised with the Image Lab software and the Universal Hood III camera system (BIO-RAD). Densitometry analysis of the bands using ImageJ was applied to calculate the intensity of the signal for each band and the results normalised to the levels of synaptophysin. Protein transfer was monitored in every case by staining the membranes with Ponceau Red.

Statistical analysis of western blot data presented in Figure 4 was carried out using Microsoft Excel (version 16.16.27). The data were not assessed for normality, no test for outliers was conducted and statistical methods were not employed to predetermine sample size. All replicates were based on a minimum of three independent neuronal differentiation. An F-test (two sample for variance) was carried out to determine whether variances were equal or unequal between H9 and A10 for each NT3 treatment concentration. The results of the F-tests are shown in Table S1, Suppl. material for all treatments and cell lines. If $p > 0.05$ a two-sample T-test was performed assuming equal variances and if $p < 0.05$ a two-sample T-test was performed assuming unequal variances (see also Table S2, Suppl. material).

2.9 | EC_{50} calculation

The EC_{50} for Trk activation was calculated based on the signal intensity of the scanned P-Trk signals triggered by NT3 at 100 pM ($n = 20$) and 400 pM NT3 ($n = 7$). These E_{max} values were divided and found to correspond to the mean P-Trk signal intensity generated by 40 pM NT3 ($n = 11$).

2.10 | Phase-contrast imaging

Phase-contrast images were captured using an Olympus CKX41 microscope with an Olympus DP21 camera.

2.11 | Immunocytochemistry

Coverslips were prepared by washing with nitric acid overnight, then washed three times with water, once with ethanol and autoclaved.

Cells grown on coverslips were washed once with PBS and fixed with 4% paraformaldehyde (Thermofisher Scientific, catalogue number: 28908) for 30 min except when stained for TrkC, in which case cells were fixed for 10 min, washed for 5 min three times with 0.1% Tween-20 (Sigma-Aldrich, catalogue number: P1379) in PBS at room temperature (22°C), and blocked for 1 h with 3% donkey serum (Sigma-Aldrich, catalogue number: D9663) and 0.1% BSA (Sigma-Aldrich, catalogue number: A7906) in 0.1% Tween-20/PBS and incubated for 1 h at room temperature (22°C) with any of the following antibodies: anti-β-III-tubulin (Tuj1) mouse polyclonal (Abcam, mAB, catalogue number: ab78078) diluted 1:1000, goat polyclonal anti-TrkB (R&D Systems, pAB, catalogue number: AF1494) diluted 1:2000, or rabbit monoclonal anti-TrkC (Cell Signalling, mAB, catalogue number: 3376) diluted 1:2000. Subsequently, the cultures were incubated for 1 h at room temperature (22°C) with the corresponding secondary antibodies (Alexa fluor 488 donkey anti-rabbit, Alexa fluor 488 donkey anti-goat and Alexa fluor 488 donkey anti-mouse; Invitrogen, catalogue numbers: A21206, A11055, A21202). Cells were then washed for 5 min three times with 0.1% Tween-20 in PBS at room temperature (22°C) before incubation with DAPI (Sigma-Aldrich, catalogue number: D9542) in PBS (1:10000). Cells were washed once with PBS and mounted using DAKO mounting medium (Agilent, catalogue number: S3023). Coverslips were left to dry overnight before imaging with a Zeiss LSM880 Airyscan Confocal microscope.

2.12 | Cell counting

H9 TrkB-, H9 TrkC-, H9 Tuj1-, A10 TrkB-, A10 TrkC- and A10 Tuj1-positive cells were counted in 20 randomly selected fields, two coverslips, each using a Nikon Eclipse Ni-U epifluorescence microscope at 40X magnification. The number of TrkB- or TrkC-positive cells was found not to be significantly different from the number of Tuj1-positive cells, neither for H9 (TrkB, TrkC) nor A10 (TrkC) neurons.

3 | RESULTS

3.1 | Expression of the neurotrophin receptors NTRK2 and NTRK3 and generation of hESC clones lacking TrkB receptors

We previously described the effects of TrkB ligands on neurons derived from hESCs and the publicly available RNAseq data collected in these previous experiments indicated that *NTRK3*, unlike *NTRK1* and *NGFR*, was also expressed at significant levels (Merkouris et al., 2018). To quantify relative receptor expression in the neurons used in the present study, the levels of *NTRK3* were compared with those of *NTRK2* by qPCR and the results normalised to those of *GAD1*, *GAD2*, *TBP and GAPDH* (Figure 1a). As the ability of NT3 to activate TrkB is abundantly documented (Barbacid, 1994) and neurons lacking TrkB were generated by targeting with CRISPR/Cas9 Exon V of *NTRK2* in hESCs (Figure 1b). This exon contains the initiation codon of human TrkB (Luberg et al., 2010). Several clones were isolated based on the size of the predicted genomic DNA fragments and three such clones, designated A10, B1 and D2, were selected and sequenced. Control clones that went through the FACS selection procedure, but turned out not to be successfully targeted at the *NTRK2* locus were also isolated and used in control experiments, including one designated C9. The absence of TrkB protein in neurons derived from targeted clones in A10 was verified using TrkB antibodies as well as pan-Trk antibodies (Figure 1c).

3.2 | Quantification of TrkC expression by A10 neurons and of TrkB by H9 neurons

The expression of Trk receptors in A10 and H9 neurons was visualised by immunofluorescence cytochemistry (Figure 2). To this end, A10 or H9 progenitors were plated at low density on coverslips and analysed for receptor expression using a previously validated monoclonal TrkC antibody (Takahashi et al., 2011). The results revealed similar, punctate-type staining (see Figure 3 in Takahashi et al., 2011) as seen with the TrkB antibody on H9 neurons, including the staining of all neuronal processes. The absence of any TrkB antibody staining on A10 neurons substantiates the deletion of TrkB in these neurons (Figure 2). Quantification of these results (Figure 2, legend) indicated that all A10 neurons expressed TrkC and none expressed TrkB. Using Tuj1 immunoreactivity as a label for neurons and their processes, all H9 neurons were found to express TrkB. Low-magnification (20×) phase-contrast pictures of fixed H9 and A10 neurons are also included to illustrate the morphology of fixed cells visualised by phase-contrast and examples of dead cells contributing to DAPI-positive nuclei are indicated by red arrows.

3.3 | TrkB cannot be ligand activated in A10 neurons

Trk activation by NT3 was monitored with a phospho-tyrosine monoclonal antibody that does not distinguish between activated TrkB and TrkC as it targets the same residues in both receptors. It was therefore important to demonstrate the absence of any P-Trk signal following exposure of A10 neurons to BDNF (Figure 3). In addition, a previously characterised TrkB activating agonist antibody (designated ZEB85) was used as a further control (Merkouris et al., 2018). In the course of these experiments, we observed that the TrkB polyclonal antibodies used to detect TrkB on Western blots also *activate* TrkB. Figure 3 illustrates the absence of any P-Trk signal following exposure of A10 neurons to any of these three TrkB activators, whereas NT3 produced a robust P-Trk signal (left panel). The same results were obtained using neurons generated from the successfully

targeted clones B1 and D2 (see Figure 1b for the predicted protein sequences of the successfully targeted clones): a robust P-Trk signal following the addition of NT3 and no response with BDNF. The same three TrkB activators used at the same concentrations as with A10 neurons robustly activated TrkB phosphorylation in control, TrkB-expressing H9 neurons (Figure 3, right panel).

3.4 | NT3 activates TrkC at picomolar concentrations in A10 neurons and TrkB at higher concentrations in H9 neurons

The intensity of the P-Trk signal was quantified after exposing either A10 neurons (expressing only TrkC) or H9 neurons

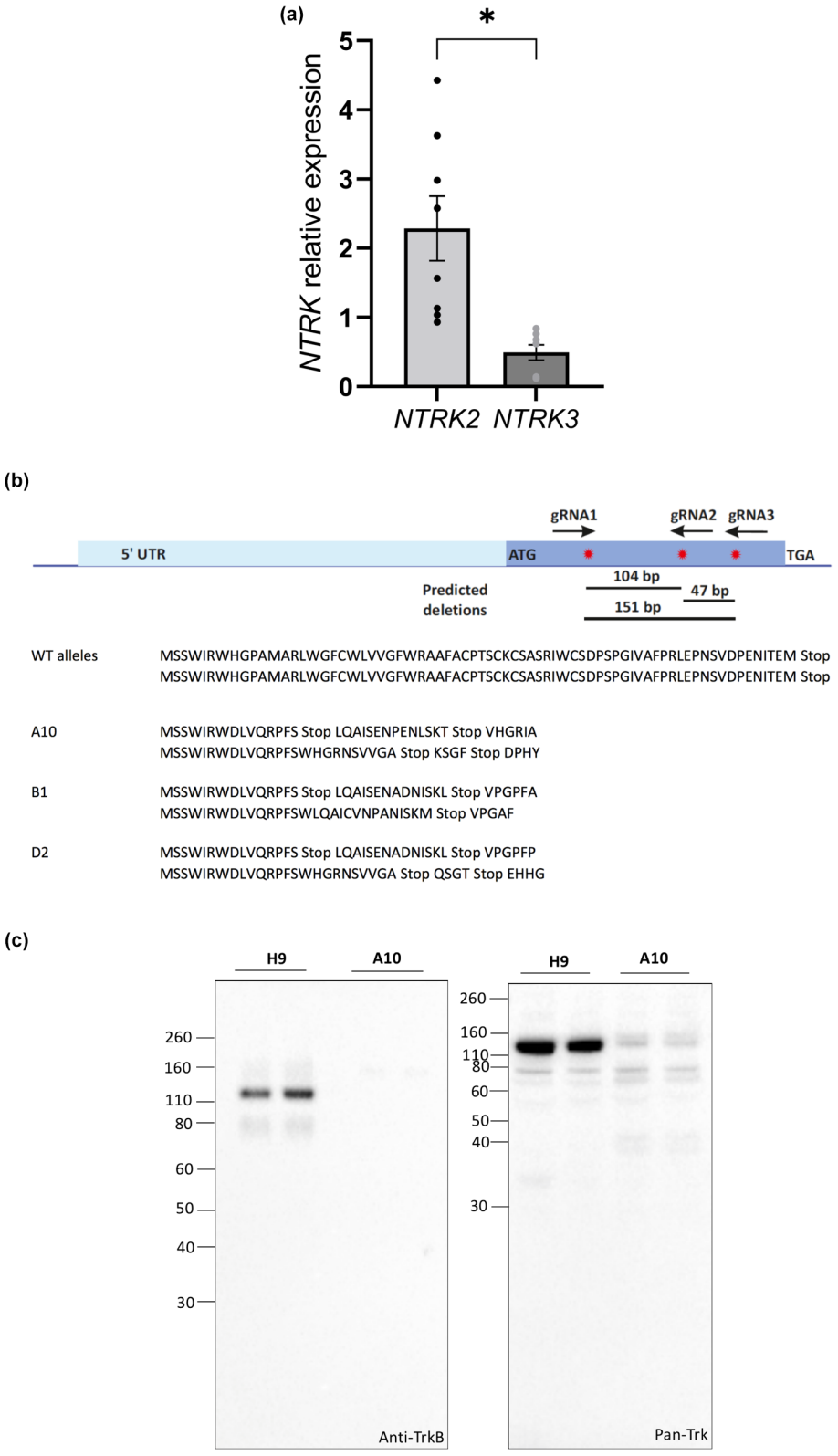

FIGURE 1 NTRK2 and NTRK3 expression in H9 neurons and generation of cells lacking TrkB. (a) NTRK2 and NTRK3 mRNA expression by H9 neurons. RT-qPCR following RNA extraction from H9 neurons shows higher expression of *NTRK2* mRNA relative to *NTRK3*. The results are normalised based on the expression of four genes: *GAD1*, *GAD2*, *GAPDH* and *BTP*. Error bars refer to SEM and $n = 8$ for each gene. All values were normalised to *GAD1*, *GAD2*, *GAPDH and BTP* expression and * corresponds to $p > 0.05$. (b) Generation of independent clones lacking TrkB by targeting the first protein coding exon. Illustration showing the predicted deletions of exon V of *NTRK2* (Luberg et al., 2010) and the three guide RNAs (gRNAs) used for the CRISPR-Cas9 targeting and the predicted N-terminal sequence of TrkB based on the nucleotide sequences determined for clones that remained untargeted (C9, AKA WT) and for each allele of the knockout clones A10, B1 and D2. (c) Lack of significant expression of TrkB by A10 neurons. Western blots for Trk protein were performed with lysates of A10 neurons. Blots were probed either with TrkB antibodies (left panel) or with pan-Trk antibodies (right panel). Note that the latter exaggerates the difference between the levels of TrkB and TrkC expression owing to their stronger reactivity with TrkB compared with TrkC

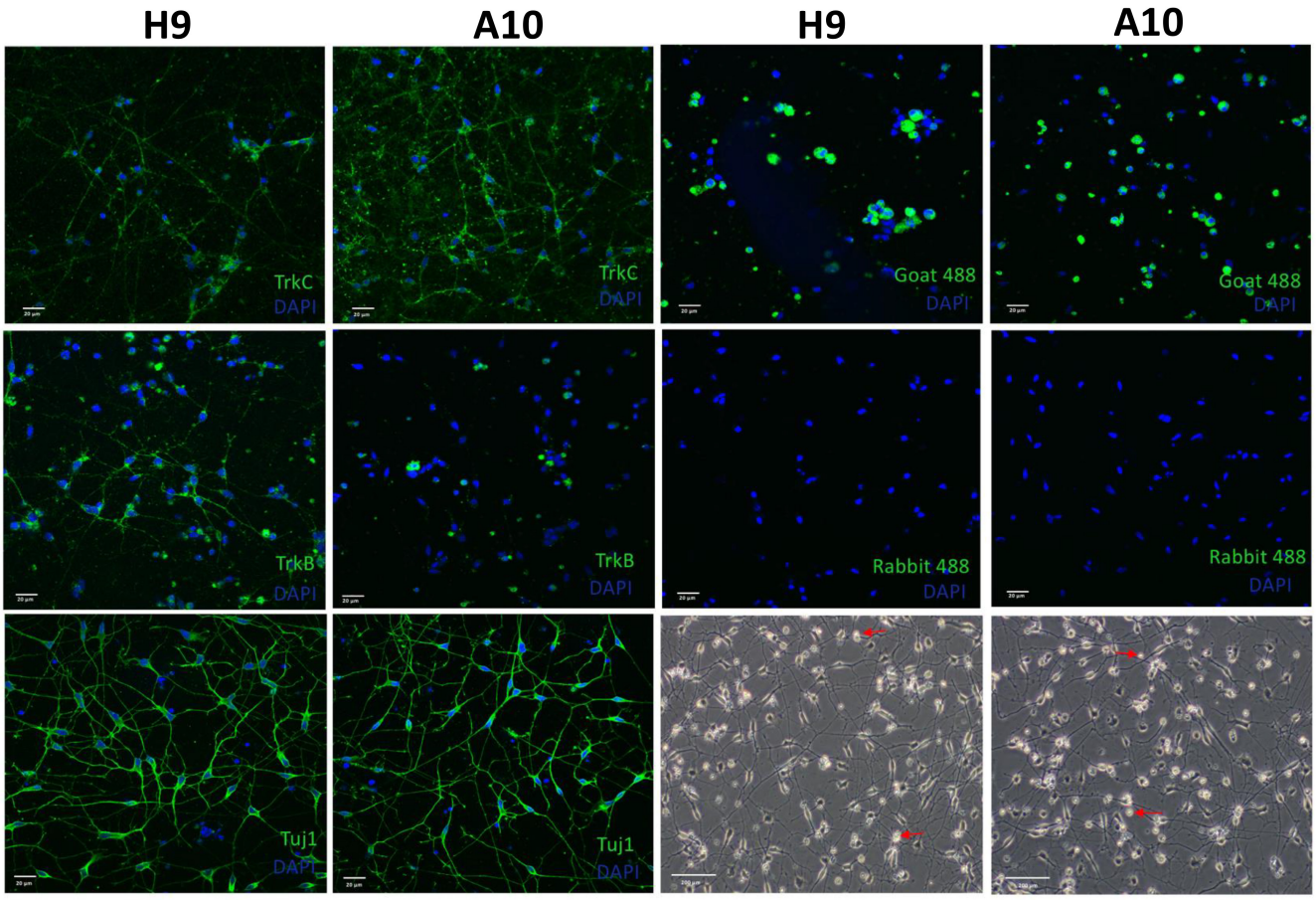

FIGURE 2 Immunostaining of H9 and A10 neurons. TrkB, TrkC and Tuj1 immunostaining of H9 and A10 neurons. Rabbit 488 and Goat 488 secondary antibody controls were obtained by omitting incubation with the primary antibodies. Note that the goat secondary antibody showed a strong background staining primarily over cell bodies. A10 neurons did not show any staining of neuronal processes with the TrkB antibody. Apparent cell body staining was also seen with the anti-goat secondary antibody only. The mean numbers ± SEM of Tuj1-positive neurons were 72.9 ± 3.1 and 72.8 ± 1.6 for H9 and A10 cells, respectively, 68.9 ± 1.9 and 73.7 ± 2.0 for H9 and A10 neurons stained with TrkC, and 72.7 neurons with TrkB. Twenty random fields were counted in each case using two different coverslips. Low magnification, phase-contrast images of H9 and A10 neurons illustrate examples of neuronal cultures at 30 days and the red arrows point to DAPI-positive dead cells. Scale bar is 20 μm for immunostaining images and 200 μm for phase-contrast images

expressing both TrkB and TrkC to increasing concentrations of NT3 for 1 h (Figure 4a–c). The P-Trk signal elicited by NT3 was found to saturate at 100 pM with the A10 neurons (Figure 1c, grey bars). By contrast, with H9 neurons the P-Trk signal markedly increased at NT3 concentrations above 100 pM (Figure 1c, black bars) as a result of TrkB activation and of the higher levels of TrkB expression in these neurons compared to TrkC (see Figure 1a).

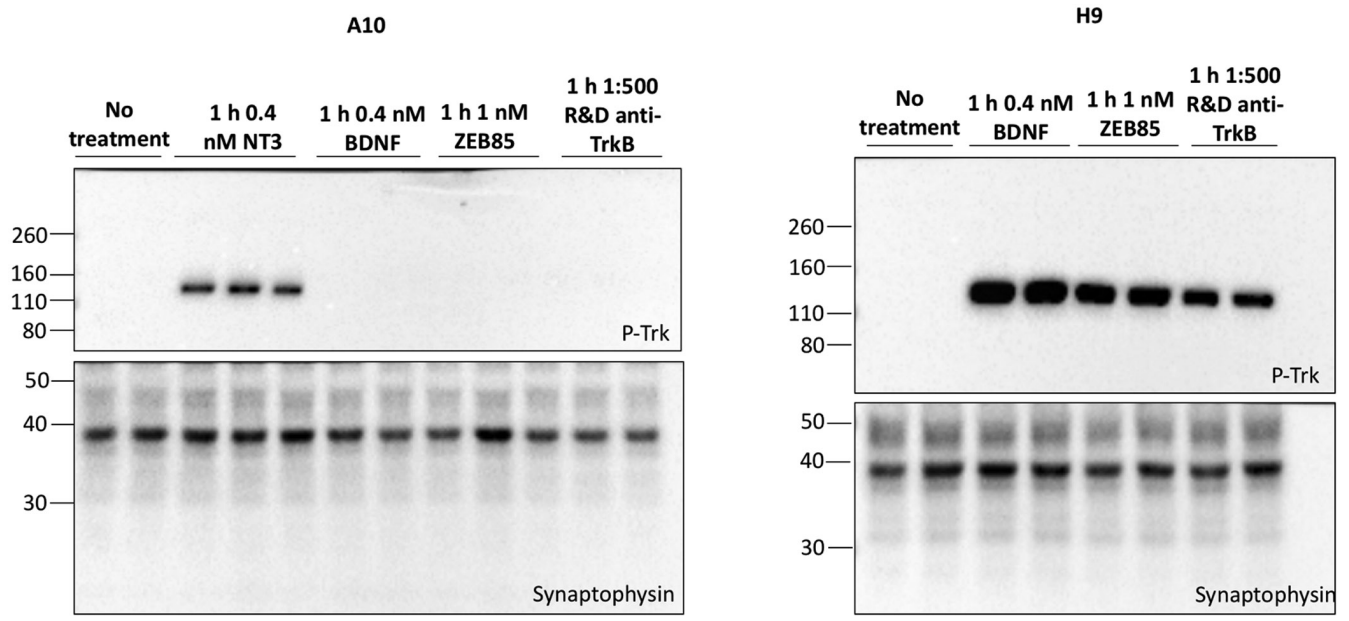

FIGURE 3 Activation of TrkC and not of TrkB in A10 neurons. Western blots for phosphorylated Trk protein (P-Trk) and synaptophysin were performed using lysates of A10 neurons (left panel) and H9 neurons (right panel). Left panel: BDNF, TrkB-activating antibody ZEB85 and the TrkB polyclonal antibodies used for Western blot (Figure 1) and immunostaining (Figure 2) all failed to generate any detectable Trk phosphorylation signal in A10 neurons while NT3 did. Right panel: The same three TrkB activators used in the left panel at the same concentrations all induced a robust Trk phosphorylation signal. All treatments were for 1 h

3.5 | Transcriptional changes caused by TrkC activation and comparison with TrkB

As all A10 neurons were found to express TrkC, we then explored the changes in the transcriptional profile caused by NT3 activation of TrkC and compared the results with those of a previous study with H9 neurons (Merkouris et al., 2018). RNA was extracted from untreated A10 cells or untreated H9 cells (0 h) or from A10 cells treated with 2 nM NT3 for 2 or 24 h. In untreated neurons, the genes expressed in common between A10 and H9 neurons were compared and amongst 14 824 genes included in this comparison, only 695 and 589 were found to be differentially expressed in A10 neurons and H9 neurons, respectively, with absolute fold- changes >2 and padj <0.01 using the limma voom algorithm of Bioconductor R package. The transcriptional changes induced by NT3 addition at 2 and 24 h are available on the EBI Website: E-MTAB 11566 and can be compared with those induced by BDNF in H9 neurons (E-MATB 6975). With few exceptions, the transcriptional changes caused by NT3 in TrkC-expressing neurons were strikingly similar to those caused by BDNF (red dots, Figure 5) and related ligands such as NT4 in TrkB-expressing neurons (Merkouris et al., 2018). The magnitude of the changes caused by NT3 was however smaller than those caused by the addition of TrkB ligands to H9 neurons, presumably reflecting the higher levels of expression of TrkB in these neurons compared with TrkC (see Figure 1a). These changes included numerous genes known to be involved in synaptic plasticity (dark bars) such as Arc/Arg3.1, a prominent representative of such genes (Zhang & Bramham, 2021). To validate Arc/Arg 3.1 expression at the protein level, lysates of A10 or H9 neurons treated with NT3 or BDNF, respectively, were assessed by Western blot analysis for Arc/Arg3.1 protein levels. In both cases, these levels were found to be markedly increased (Figure 6).

3.6 | Activation and loss of the NT3-induced P-Trk signal in A10 neurons

We next sought to determine if the widely reported desensitisation of TrkB (see "Discussion" section) in neurons exposed to saturating concentrations of BDNF would also be observed with NT3-TrkC signalling. A10 neurons were exposed to saturating concentrations of NT3 and the levels of the P-Trk signal were examined at different time points. We found that the P-Trk signal had essentially disappeared 6 h post-treatment (Figure 7a). This is reminiscent of previous observations with H9 neurons indicating the loss of P-Trk signal following exposure of neurons to TrkB ligands used at saturating concentrations (Merkouris et al., 2018). Importantly, the loss of P-Trk signal was accompanied by a marked reduction of the levels of TrkC protein (Figure 7a).

3.7 | Down-regulation of TrkB by BDNF does not impact TrkC activation by NT3

We next examined whether exposing H9 neurons to saturating concentrations of BDNF would impair a subsequent response to NT3 (Figure 7b). Following incubation of H9 neurons for 24 h with 1 nM BDNF, activation of TrkC by NT3 remained intact in a

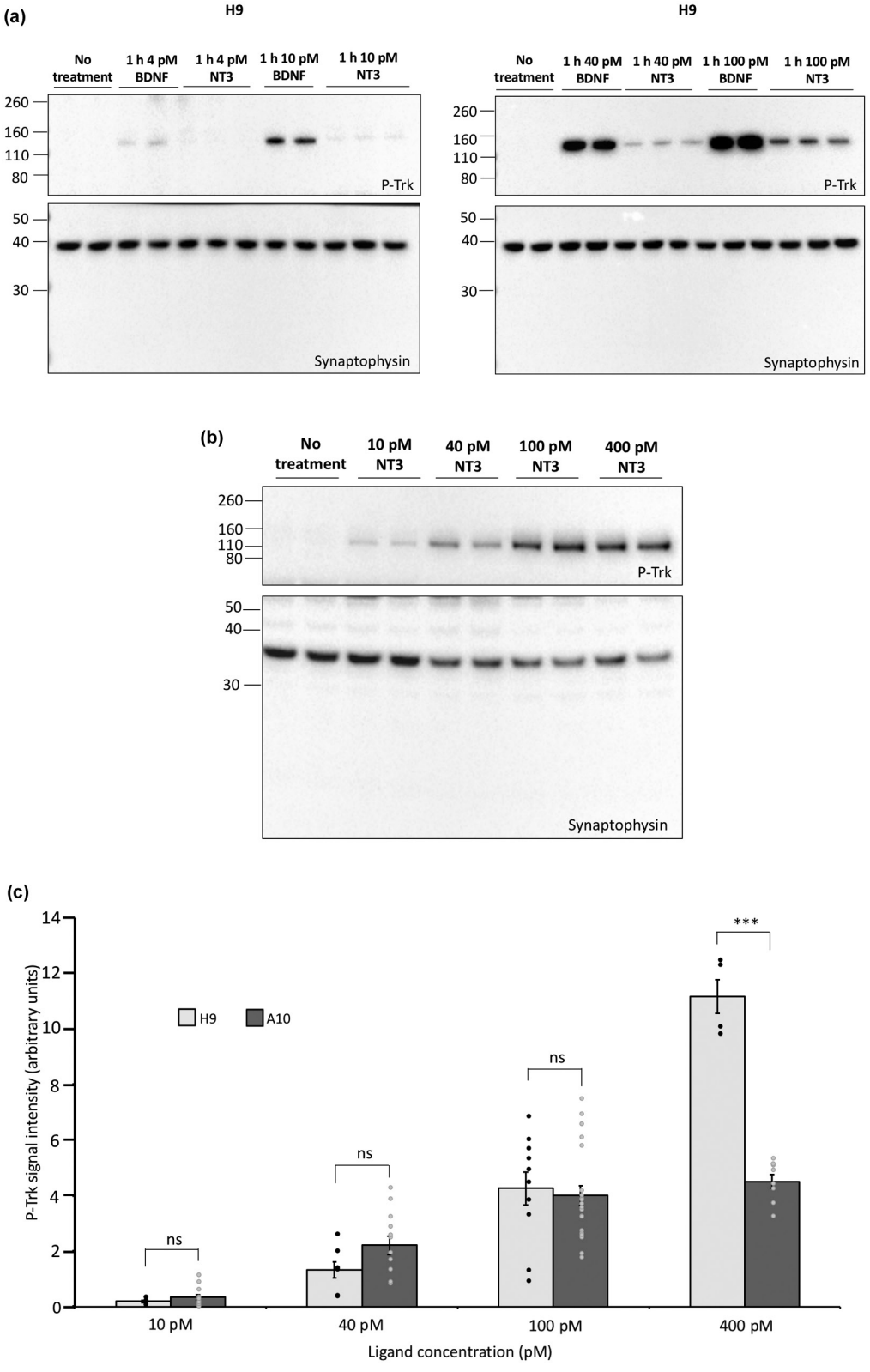

FIGURE 4 P-Trk response to NT3 in H9 and A10 neurons. (a) BDNF and NT3 P-Trk dose–response. Western blots for phosphorylated Trk receptor (P-Trk) and synaptophysin using lysates of H9 neurons treated with either low (left panel) or high (right panel) concentrations of BDNF and NT3. (b) P-Trk dose–response in A10 neurons. Western blot for phosphorylated Trk receptor (P-Trk) and synaptophysin using lysates of A10 neurons treated with increasing concentrations of NT3. (c) Quantification of P-Trk in H9 and A10 neurons. Densitometric analysis of P-Trk activation in H9 and A10 neurons at the NT3 concentrations indicated. Treatments were for 1 h. The error bars refer to SEM and significance indicated with asterisks: $^{***}p < 0.001$ and ns refers to $p > 0.05$. For H9, 10 pM NT3 $n = 7$, 40 pM NT3 $n = 7$, 100 pM NT3 $n = 10$, 400 pM NT3 $n = 4$. For A10, 10 pM NT3 $n = 12$, 40 pM NT3 $n = 11$, 100 pM NT3 $n = 20$, 400 pM NT3 $n = 8$

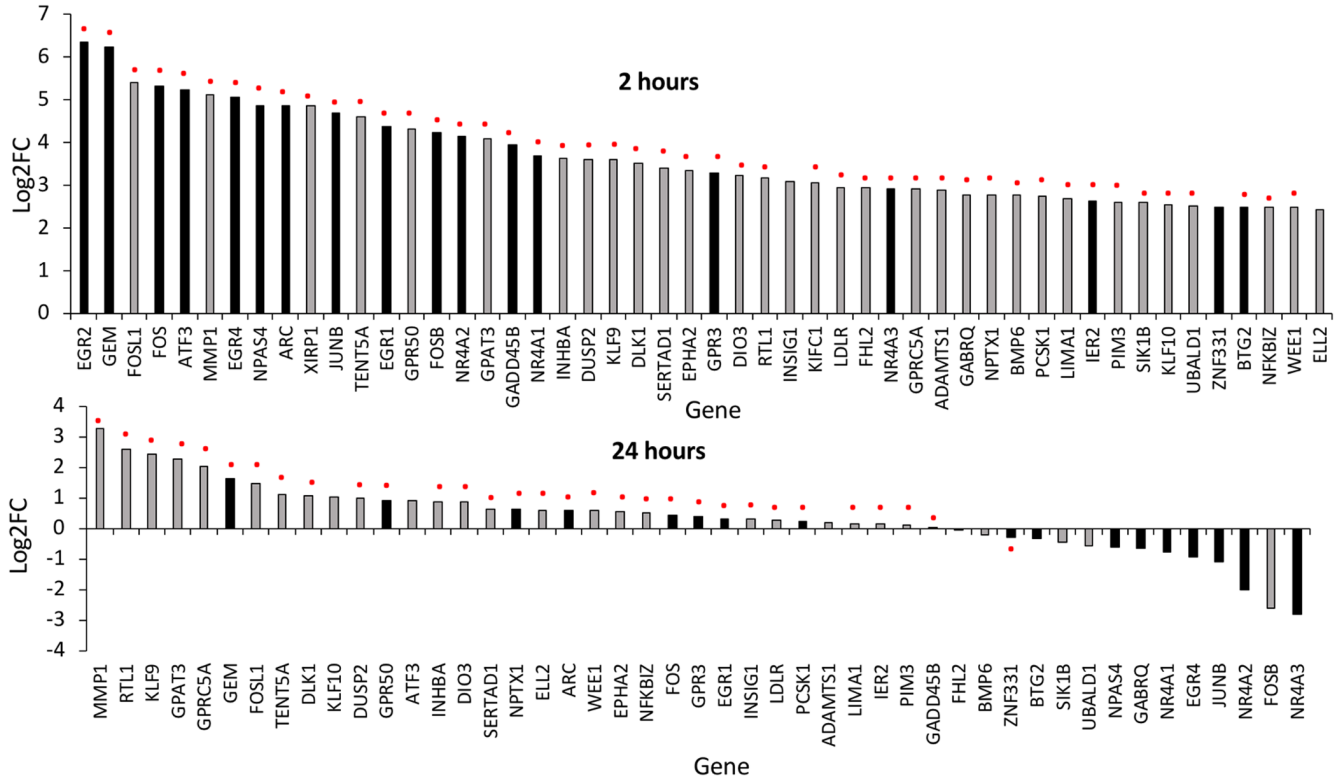

FIGURE 5 Comparison of gene expression changes caused by NT3 addition to A10 neurons and comparison with BDNF addition to H9 neurons. Genes most induced or repressed by NT3 at 2 h (top) and 24 h (bottom) were ranked by log2 fold changes with padj <0.01. For additional details, see E-MTAB 11566. Black bars indicate genes belonging to a core set of synaptic plasticity genes regulated by neuronal activity in human neurons (Pruunsild et al., 2017). Red dots indicate genes also induced or repressed by BDNF treatment in H9 neurons

concentration-dependent manner. Taken together with the observation that NT3 activates TrkC at pM concentration in A10 neurons, these results confirm the notion that NT3 can signal through TrkC in human neurons immaterial of the presence or absence of TrkB expression (see Figure 3 and Figure 7b). A control experiment confirmed that TrkB could not be reactivated by 1 nM BDNF re-added after 24 h (Figure 7b, left panel). In addition, TrkB protein is no longer detectable (Figure 7b, right panel).

3.8 | Sub-saturating concentrations of BDNF do not down-regulate TrkB and allow TrkB reactivation

We next examined if lower, more physiological concentrations of BDNF (see Introduction) would allow reactivation of TrkB upon subsequent stimulation of neurons with BDNF. H9 neurons were exposed for 24 h to a sub-saturating concentration of BDNF (40 pM) and then re-exposed 24 h later to the same 40 pM concentration. The analysis of the corresponding lysates probed with P-Trk antibodies revealed that under these conditions, TrkB could indeed be reactivated (Figure 8, left panel) and TrkB protein was still detectable (Figure 8, right panel). Note that this was not the case when H9 neurons were exposed to saturating concentrations of BDNF (Figure 7b).

4 | DISCUSSION

Our results reveal that TrkC activation by NT3 can occur in neurons where TrkB has been down-regulated following exposure to high concentrations of BDNF, thus arguing for independent signalling pathways. They also show that TrkC activation triggers transcriptional changes similar to those caused by TrkB activation whereby the use of mutant neurons excluded the possibility that these changes may result from TrkB activation by NT3. Ligand-induced loss of TrkB signalling has been previously observed not only in vitro but also in vivo following injections of large doses of BDNF (Arevalo et al., 2006; Chen et al., 2005; Frank et al., 1996; Frank et al., 1997; Knusel et al., 1997; Sommerfeld et al., 2000). Similarly here, saturating levels of either BDNF or NT3 not only prevented their respective receptor reactivation but also decreased the levels of the cognate receptors to minimal levels for 24 h. By contrast, initial TrkB activation by low BDNF concentrations allowed TrkB reactivation following re-exposure of neurons to BDNF at 24 h. Most previous studies, including our own, that examined the effects of neurotrophins on cultured neurons have been conducted using supra-saturating concentrations of neurotrophins, typically 1 or 2 nM. In light of our new results indicating that BDNF concentrations more likely to be in a physiological range did allow receptor reactivation, it would be important to reconsider preclinical studies using lower neurotrophin concentrations. Interestingly, it has been previously noted that the mode of administration of BDNF

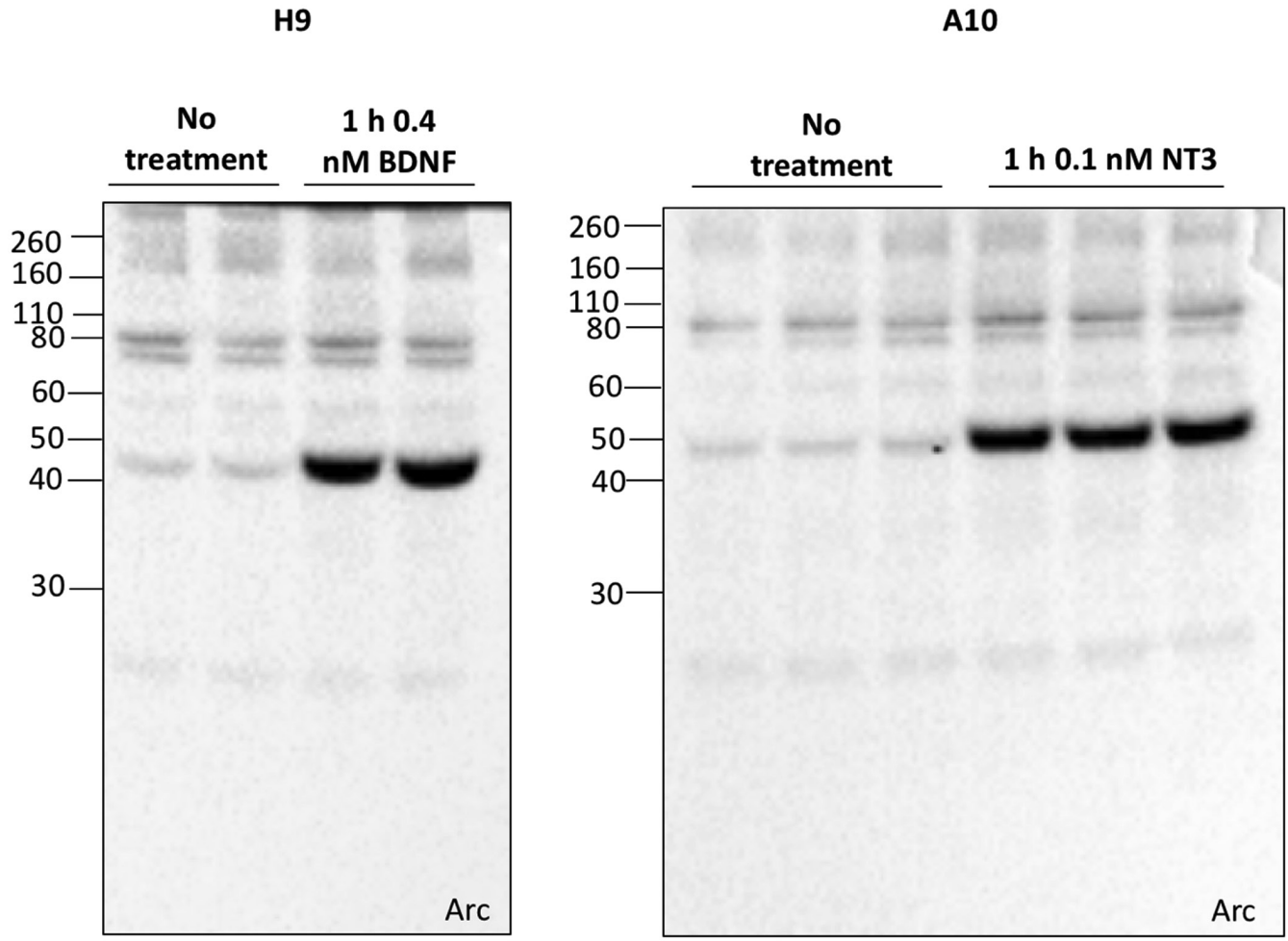

FIGURE 6 Induction of arc/Arg3.1 protein by TrkB and TrkC activation. Western blots for arc/Arg3.1 were performed on lysates of H9 and A10 neurons treated with BDNF or NT3 for 1 h as indicated show that arc/Arg3.1 is induced by BDNF-mediated TrkB activation and NT3-mediated TrkC activation

alters the type of response mediated by TrkB activation. In particular, a progressive increase in the concentration of BDNF to a final concentration of 1 nM, as opposed to the acute delivery of BDNF at the same concentration, has been reported to initiate a more sustained activation of TrkB (Ji et al., 2010). Similar differential effects were noted in the same study with regard to the levels of Arc/Arg3.1 (Ji et al., 2010). Similarly, repeated bolus BDNF injections into the hippocampus have been shown to elicit different effects compared with continuous BDNF administration through a mini-pump (Xu et al., 2004). These results emphasise the importance of re-examining dose level and dose frequency when attempting to observe the biological effects of neurotrophins. Our observations suggest that, compared to several studies conducted in the past, the use of much lower concentrations of Trk agonists may lead to more robust outcomes than has been observed in the past when using neurotrophins to treat neurodegenerative conditions (Thoenen & Sendtner, 2002).

Cultured neurons differentiated from hESCs turned out to express neurotrophin receptors in a pattern surprisingly similar to what has been established by brain-wide RNAseq studies, i.e. co-expression of TrkB and TrkC by single neurons, at a ratio mirroring the situation in most brain areas (Figure S1). In addition, the NGF receptor *NTRK1* and the neurotrophin receptor p75 *NGFR* were confirmed in the present study to be expressed at negligible levels in hESC-derived neurons (Merkouris et al., 2018), as is the case in most brain areas, with few exceptions such as the basal forebrain cholinergic neurons (Volosin et al., 2006). These observations are noteworthy as the differentiation protocol used here does not select for neurons with a particular pattern of neurotrophin receptor expression. Specifically, TrkB activators such as BDNF, typically used in this type of culture protocol (Telezhkin et al., 2016), were not included. This striking pattern of neurotrophin receptor expression may be a consequence of an intrinsic and robust developmental programme unfolding in a coordinated fashion during the course of neuronal differentiation. All that may be required to mimic this pattern during hESC differentiation are permissive tissue culture conditions.

Of special relevance to the main objectives of this study, namely the characterisation of TrkC activation by NT3, was the finding that the levels of TrkB expression were significantly higher than those of TrkC, as is the case in most brain regions. The elimination of TrkB revealed that TrkC can be activated at pM concentrations of NT3,

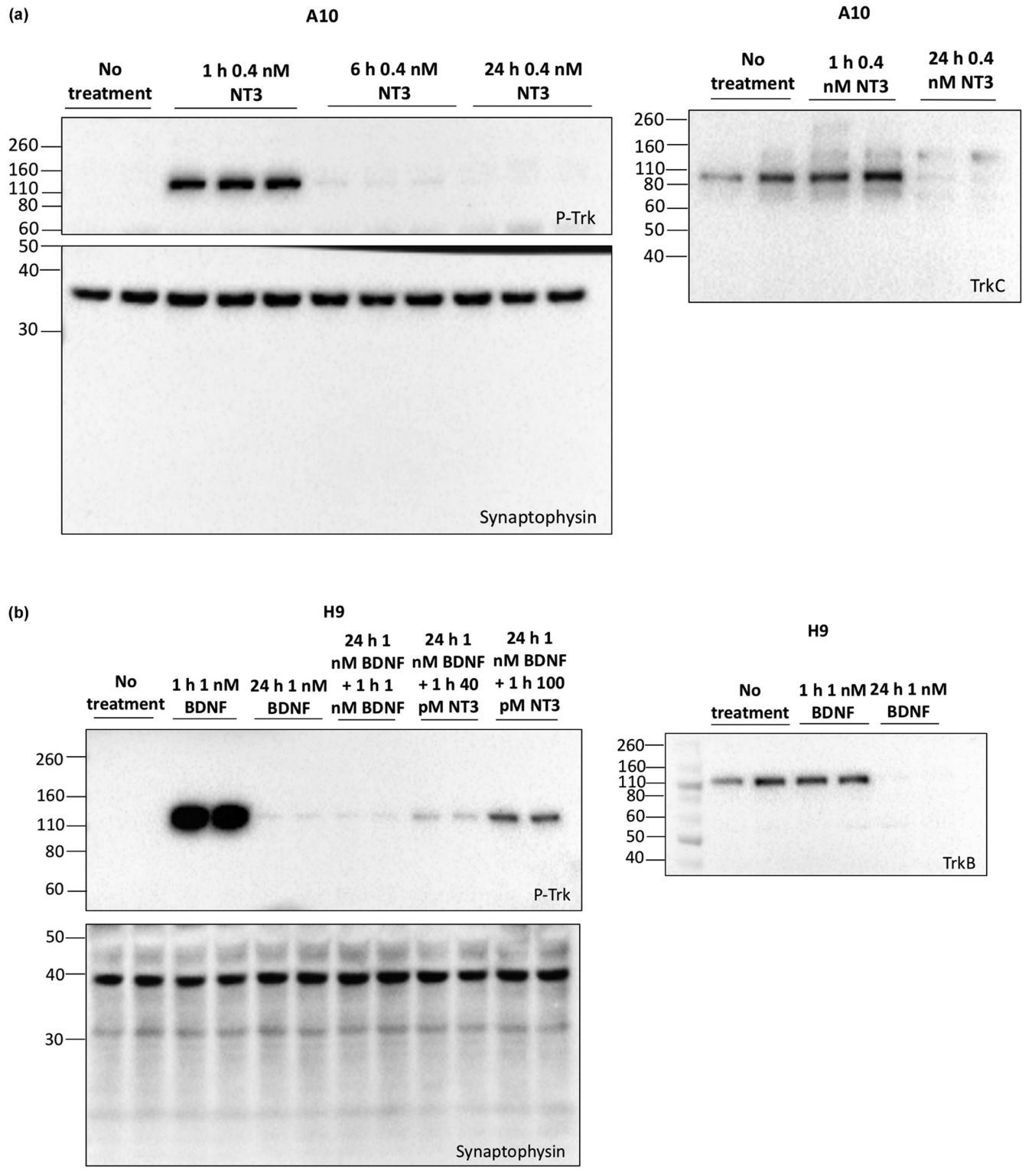

FIGURE 7 Loss of Trk following prolonged exposure to neurotrophins. (a) Loss of TrkC following 24 h exposure of A10 neurons to NT3. Western blots for phosphorylated Trk protein (P-Trk), TrkC and synaptophysin were performed with lysates of A10 neurons treated with 400 pM NT3. Note that the loss of phosphorylation signal after 24 h NT3 (left panel) is accompanied by a reduction in TrkC protein (right panel). (b) Loss of TrkB following 24 h exposure of H9 neurons to BDNF and rescue of the Trk phosphorylation signal by NT3. Western blots for phosphorylated Trk protein (P-Trk), TrkB and synaptophysin (as indicated) were performed on lysates of H9 neurons treated with BDNF and NT3 (as indicated). Note that the loss of phosphorylation after 24 h BDNF (left panel) is not rescued by re-exposure to BDNF and is accompanied by a reduction in TrkB protein (right panel). The loss of TrkB following 24 h exposure to BDNF did not impact the NT3-induced phosphorylation of TrkC

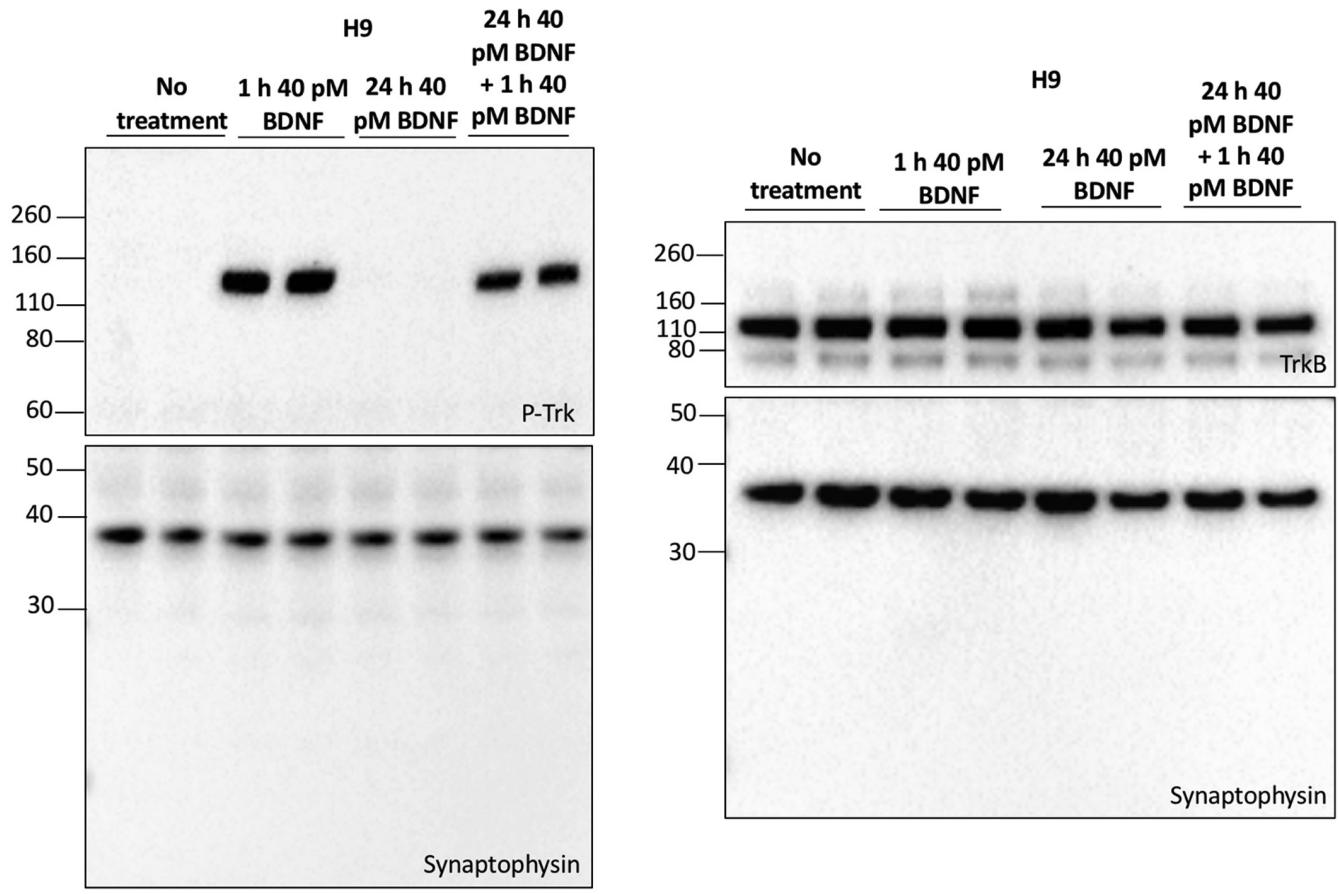

FIGURE 8 Phosphorylation of TrkB following prolonged exposure of H9 neurons to low concentrations of BDNF can be recovered upon re-exposure to BDNF. Western blots for phosphorylated Trk protein (P-Trk), TrkB and synaptophysin with lysates of H9 neurons treated with BDNF (as indicated). Note that when lower BDNF concentrations are used (40 pM), TrkB can be reactivated after 24 h (left panel) and TrkB protein levels are not decreased (right panel)

immaterial to the presence or absence of TrkB expressed by the same neurons. Importantly, the EC_{50} calculated for TrkC activation by NT3 was lower than for TrkB activation by BDNF in the same system, that is 40 pM NT3 versus 190 pM for BDNF (Merkouris et al., 2018). These characteristics of NT3 activation of TrkC have been difficult to establish thus far given that the expression of Trk receptors in heterologous system alters the properties of Trk receptor activation. In particular, Trk receptor affinity for neurotrophins is notably lower in such systems as shown by direct binding studies (Rodriguez-Tebar et al., 1991). In addition, the ligand selectivity of Trk receptors is less rigorous, especially in the case of TrkB and its activation by NT3. In heterologous systems, TrkB can be activated by NT3 at concentrations similar to BDNF (Barbacid, 1994).

The finding that NT3 activates TrkC at very low, likely physiologically relevant concentrations helps to explain the functional role of NT3/TrkC signalling in the developing cerebellum. Using an elegant single-cell marking technique allowing isolated, labelled mutant cells to be identified amongst wild-type siblings, Joo and colleagues demonstrated that the loss of TrkC in single Purkinje cells impairs the growth of their dendrites (Joo et al., 2014). This work also revealed that these dendrites compete with their wild-type neighbours as the elimination of TrkC in all Purkinje cells failed to reveal a phenotype with regard to dendritic growth. The same study also demonstrated that this phenomenon depends on the provision of NT3 delivered by Purkinje cells afferents, the cerebellar granule cells (Joo et al., 2014). This is reminiscent of the observation that the loss of BDNF in single neurons impairs their dendritic arborisation in the cerebral cortex when these neurons are surrounded by wild-type neurons (English et al., 2012). The results related to the in vivo relevance of the NT3/TrkC signalling system are not only remarkable as such but also of direct relevance to our study as Purkinje cells also express TrkB in addition to TrkC and cerebellar granule cells are a major site of not only NT3 but also of BDNF expression (Carter et al., 2002).

A possible explanation for the benefit of this dual signalling system involving BDNF/TrkB and NT3/TrkC in the same neurons may lie in the distinct regulation of *BDNF* and *NTF3* expression. Whilst the expression of *BDNF* is well known to be regulated by neuronal activity (West et al., 2002) such is not the case with *NTF3* (Hernandez-Echeagaray, 2020). The genomic organisation of *NTF3* is much less complex than BDNF (West et al., 2014) and the levels of *NTF3* are regulated by hormones such as thyroxin, rather than by neuronal activity (Lindholm et al., 1993). Downstream of Trk activation, the results of the RNAseq experiments indicated that the transcriptional

changes caused by TrkB or TrkC activation largely overlap. Most of the differences are quantitative in nature, presumably reflecting the higher levels of expression of TrkB compared with TrkC. In particular, fewer changes in gene expression levels were noted 24 h following TrkC activation, compared with TrkB activation. Beyond its ability to selectivity bind NT3, TrkC has also been discovered to partner with the axonal protein phosphatase receptor-designated PTPσ, and to trigger the differentiation of neurotransmitter release sites in excitatory terminals (Takahashi et al., 2011). Whilst PTPσ binding does not involve the NT3 binding site on TrkC, NT3 does modulate this synaptic organising function of TrkC in concert with PTPσ, in a concentration-dependent manner (Han et al., 2016). No data of sufficiently high resolution are available on the distribution of TrkC on the neuronal surface but it is conceivable that a restricted distribution of TrkC facing pre-synaptic terminals delivering NT3 may also impact the selectivity of receptor activation.

In conclusion, our results indicate NT3 activates TrkC at pM concentrations, in line with the notion that in vivo, neurotrophins are only available in limited amounts. The exquisite sensitivity of TrkC likely explains how NT3 can transduce its own growth-promoting effects, despite the co-expression of TrkB and TrkC by most CNS neurons. As our findings also indicate that Trk receptors can be reactivated following their exposure to low, presumably physiologically relevant neurotrophin concentrations, it may be useful in future experiments to use this knowledge when considering neurotrophin-based therapies.

AUTHOR CONTRIBUTIONS

S.A. performed all the cell culture and most of the biochemical experiments, S.M. helped with RNAseq data analysis, S.W. with the qPCR experiments, N.D.A. designed the CRISPR strategy, J.X. provided the CHO Trk lines, S.A., S.M., S.W., Y.-A.B., P.S.D. and R.M.L. analysed the results, S.A., S.W., N.D.A., P.S.D., R.M.L. and Y.-A.B. planned the research, S.A., S.W., N.D.A., R.M.L. and Y.-A.B. wrote the manuscript.

ACKNOWLEDGEMENTS

The authors wish to thank Angela Marchbank for her help with the RNAseq experiments and Bridget Allen for kindly sharing reagents and her assistance with the CRISPR/Cas9 process. ARRIVE guidelines were not followed since they do not apply to this study.

DATA AVAILABILITY STATEMENT

RNAseq data are publicly accessible at https://www.ebi.ac.uk/arrayexpress/experiments/E-MTAB-11566/ under ID: E-MTAB-11566.

ORCID

Sean Wyatt https://orcid.org/0000-0002-0572-234X
Yves-Alain Barde https://orcid.org/0000-0002-7627-461X

REFERENCES

Arevalo, J. C., Waite, J., Rajagopal, R., Beyna, M., Chen, Z. Y., Lee, F. S., & Chao, M. V. (2006). Cell survival through Trk neurotrophin receptors is differentially regulated by ubiquitination. *Neuron*, *50*, 549–559.

Barbacid, M. (1994). The Trk family of neurotrophin receptors. *Journal of Neurobiology*, *25*, 1386–1403.

Bibel, M., Richter, J., Lacroix, E., & Barde, Y.-A. (2007). Generation of a defined and uniform population of CNS progenitors and neurons from mouse embryonic stem cells. *Nature Protocols*, *2*, 1034–1043.

Bibel, M., Richter, J., Schrenk, K., Tucker, K. L., Staiger, V., Korte, M., Goetz, M., & Barde, Y.-A. (2004). Differentiation of mouse embryonic stem cells into a defined neuronal lineage. *Nature Neuroscience*, *7*, 1003–1009.

Bruntraeger, M., Byrne, M., Long, K., & Bassett, A. R. (2019). Editing the genome of human induced pluripotent stem cells using CRISPR/Cas9 ribonucleoprotein complexes. *Methods in Molecular Biology*, *1961*, 153–183.

Carter, A. R., Chen, C., Schwartz, P. M., & Segal, R. A. (2002). Brain-derived neurotrophic factor modulates cerebellar plasticity and synaptic ultrastructure. *The Journal of Neuroscience*, *22*, 1316–1327.

Chen, Z. Y., Ieraci, A., Tanowitz, M., & Lee, F. S. (2005). A novel endocytic recycling signal distinguishes biological responses of Trk neurotrophin receptors. *Molecular Biology of the Cell*, *16*, 5761–5772.

Davies, A. M. (1994). The role of neurotrophins in the developing nervous system. *Journal of Neurobiology*, *25*, 1334–1348.

English, C. N., Vigers, A. J., & Jones, K. R. (2012). Genetic evidence that brain-derived neurotrophic factor mediates competitive interactions between individual cortical neurons. *Proceedings of the National Academy of Sciences of the United States of America*, *109*, 19456–19461.

Erickson, J. T., Conover, J. C., Borday, V., Champagnat, J., Barbacid, M., Yancopoulos, G., & Katz, D. M. (1996). Mice lacking brain-derived neurotrophic factor exhibit visceral sensory neuron losses distinct from mice lacking NT4 and display a severe developmental deficit in control of breathing. *The Journal of Neuroscience*, *16*, 5361–5371.

Frank, L., Ventimiglia, R., Anderson, K., Lindsay, R. M., & Rudge, J. S. (1996). BDNF down-regulates neurotrophin responsiveness, TrkB protein and TrkB mRNA levels in cultured rat hippocampal neurons. *The European Journal of Neuroscience*, *8*, 1220–1230.

Frank, L., Wiegand, S. J., Siuciak, J. A., Lindsay, R. M., & Rudge, J. S. (1997). Effects of BDNF infusion on the regulation of TrkB protein and message in adult rat brain. *Experimental Neurology*, *145*, 62–70.

Hamburger, V., Brunso-Bechtold, J. K., & Yip, J. W. (1981). Neuronal death in the spinal ganglia of the chick embryo and its reduction by nerve growth factor. *The Journal of Neuroscience*, *1*, 60–71.

Han, K. A., Woo, D., Kim, S., Choii, G., Jeon, S., Won, S. Y., Kim, H. M., Heo, W. D., Um, J. W., & Ko, J. (2016). Neurotrophin-3 regulates synapse development by modulating TrkC-PTPsigma synaptic adhesion and intracellular signaling pathways. *The Journal of Neuroscience*, *36*, 4816–4831.

Hernandez-Echeagaray, E. (2020). Neurotrophin-3 modulates synaptic transmission. *Vitamins and Hormones*, *114*, 71–89.

Hofer, M. M., & Barde, Y. A. (1988). Brain-derived neurotrophic factor prevents neuronal death in vivo. *Nature*, *331*, 261–262.

Huang, E. J., & Reichardt, L. F. (2001). Neurotrophins: Roles in neuronal development and function. *Annual Review of Neuroscience*, *24*, 677–736.

Hwang, S., Cavaliere, P., Li, R., Zhu, L. J., Dephoure, N., & Torres, E. M. (2021). Consequences of aneuploidy in human fibroblasts with trisomy 21. *Proceedings of the National Academy of Sciences*, *118*, e2014723118.

Ji, Y., Lu, Y., Yang, F., Shen, W., Tang, T. T., Feng, L., Duan, S., & Lu, B. (2010). Acute and gradual increases in BDNF concentration elicit distinct signaling and functions in neurons. *Nature Neuroscience*, *13*, 302–309.

Joo, W., Hippenmeyer, S., & Luo, L. (2014). Neurodevelopment. Dendrite morphogenesis depends on relative levels of NT-3/TrkC signaling. *Science*, *346*, 626–629.

Knusel, B., Gao, H., Okazaki, T., Yoshida, T., Mori, N., Hefti, F., & Kaplan, D. R. (1997). Ligand-induced down-regulation of Trk messenger RNA, protein and tyrosine phosphorylation in rat cortical neurons. *Neuroscience*, *78*, 851–862.

Korte, M., Carroll, P., Wolf, E., Brem, G., Thoenen, H., & Bonhoeffer, T. (1995). Hippocampal long-term potentiation is impaired in mice lacking brain-derived neurotrophic factor. *Proceedings of the National Academy of Sciences of the United States of America*, *92*, 8856–8860.

Lindholm, D., Castren, E., Tsoulfas, P., et al. (1993). Neurotrophin-3 induced by tri-iodothyronine in cerebellar granule cells promotes Purkinje cell differentiation. *The Journal of Cell Biology*, *122*, 443–450.

Luberg, K., Wong, J., Weickert, C. S., & Timmusk, T. (2010). Human TrkB gene: Novel alternative transcripts, protein isoforms and expression pattern in the prefrontal cerebral cortex during postnatal development. *Journal of Neurochemistry*, *113*, 952–964.

Merkouris, S., Barde, Y. A., Binley, K. E., Allen, N. D., Stepanov, A. V., Wu, N. C., Grande, G., Lin, C. W., Li, M., Nan, X., Chacon-Fernandez, P., DiStefano, P., Lindsay, R. M., Lerner, R. A., & Xie, J. (2018). Fully human agonist antibodies to TrkB using autocrine cell-based selection from a combinatorial antibody library. *Proceedings of the National Academy of Sciences of the United States of America*, *115*, E7023–e7032.

Patterson, S. L., Abel, T., Deuel, T. A., Martin, K. C., Rose, J. C., & Kandel, E. R. (1996). Recombinant BDNF rescues deficits in basal synaptic transmission and hippocampal LTP in BDNF knockout mice. *Neuron*, *16*, 1137–1145.

Pruunsild, P., Bengtson, C. P., & Bading, H. (2017). Networks of cultured iPSC-derived neurons reveal the human synaptic activity-regulated adaptive gene program. *Cell Reports*, *18*, 122–135.

Puehringer, D., Orel, N., Luningschror, P., Subramanian, N., Herrmann, T., Chao, M. V., & Sendtner, M. (2013). EGF transactivation of Trk receptors regulates the migration of newborn cortical neurons. *Nature Neuroscience*, *16*, 407–415.

Rauskolb, S., Zagrebelsky, M., Dreznjak, A., Deogracias, R., Matsumoto, T., Wiese, S., Erne, B., Sendtner, M., Schaeren-Wiemers, N., Korte, M., & Barde, Y. A. (2010). Global deprivation of brain-derived neurotrophic factor in the CNS reveals an area-specific requirement for dendritic growth. *The Journal of Neuroscience*, *30*, 1739–1749.

Rodriguez-Tebar, A., Dechant, G., & Barde, Y. A. (1991). Neurotrophins: Structural relatedness and receptor interactions. *Philosophical Transactions of the Royal Society of London. Series B, Biological Sciences*, *331*, 255–258.

Sommerfeld, M. T., Schweigreiter, R., Barde, Y. A., & Hoppe, E. (2000). Down-regulation of the neurotrophin receptor TrkB following ligand binding. Evidence for an involvement of the proteasome and differential regulation of TrkA and TrkB. *The Journal of Biological Chemistry*, *275*, 8982–8990.

Takahashi, H., Arstikaitis, P., Prasad, T., Bartlett, T. E., Wang, Y. T., Murphy, T. H., & Craig, A. M. (2011). Postsynaptic TrkC and presynaptic PTPsigma function as a bidirectional excitatory synaptic organizing complex. *Neuron*, *69*, 287–303.

Telezhkin, V., Schnell, C., Yarova, P., Yung, S., Cope, E., Hughes, A., Thompson, B. A., Sanders, P., Geater, C., Hancock, J. M., Joy, S., Badder, L., Connor-Robson, N., Comella, A., Straccia, M., Bombau, G., Brown, J. T., Canals, J. M., Randall, A. D., … Kemp, P. J. (2016). Forced cell cycle exit and modulation of GABAA, CREB, and GSK3beta signaling promote functional maturation of induced pluripotent stem cell-derived neurons. *American Journal of Physiology. Cell Physiology*, *310*, C520–C541.

Thoenen, H. and Sendtner, M. (2002) Neurotrophins: From enthusiastic expectations through sobering experiences to rational therapeutic approaches. *Nature Neuroscience 5* Suppl, 1046–1050.

Thomson, J. A., Itskovitz-Eldor, J., Shapiro, S. S., Waknitz, M. A., Swiergiel, J. J., Marshall, V. S., & Jones, J. M. (1998). Embryonic stem cell lines derived from human blastocysts. *Science*, *282*, 1145–1147.

Vandesompele, J., De Preter, K., Pattyn, F., Poppe, B., Van Roy, N., De Paepe, A., & Speleman, F. (2002). Accurate normalization of real-time quantitative RT-PCR data by geometric averaging of multiple internal control genes. *Genome Biology*, *3*(research0034), 0031.

Volosin, M., Song, W., Almeida, R. D., Kaplan, D. R., Hempstead, B. L., & Friedman, W. J. (2006). Interaction of survival and death signaling in basal forebrain neurons: Roles of neurotrophins and proneurotrophins. *The Journal of Neuroscience*, *26*, 7756–7766.

Wang, C. S., Kavalali, E. T., & Monteggia, L. M. (2022). BDNF signaling in context: From synaptic regulation to psychiatric disorders. *Cell*, *185*, 62–76.

West, A. E., Griffith, E. C., & Greenberg, M. E. (2002). Regulation of transcription factors by neuronal activity. *Nature Reviews. Neuroscience*, *3*, 921–931.

West, A. E., Pruunsild, P., & Timmusk, T. (2014). Neurotrophins: Transcription and translation. *Handbook of Experimental Pharmacology*, *220*, 67–100.

Xu, W., Chi, L., Row, B. W., Xu, R., Ke, Y., Xu, B., Luo, C., Kheirandish, L., Gozal, D., & Liu, R. (2004). Increased oxidative stress is associated with chronic intermittent hypoxia-mediated brain cortical neuronal cell apoptosis in a mouse model of sleep apnea. *Neuroscience*, *126*, 313–323.

Ying, Q. L., Wray, J., Nichols, J., Batlle-Morera, L., Doble, B., Woodgett, J., Cohen, P., & Smith, A. (2008). The ground state of embryonic stem cell self-renewal. *Nature*, *453*, 519–523.

Zhang, H., & Bramham, C. R. (2021). Arc/Arg3.1 function in long-term synaptic plasticity: Emerging mechanisms and unresolved issues. *The European Journal of Neuroscience*, *54*, 6696–6712.

SUPPORTING INFORMATION

Additional supporting information may be found in the online version of the article at the publisher's website.

How to cite this article: Ateaque, S., Merkouris, S., Wyatt, S., Allen, N. D., Xie, J., DiStefano, P. S., Lindsay, R. M., Barde, Y-A (2022). Selective activation and down-regulation of Trk receptors by neurotrophins in human neurons co-expressing TrkB and TrkC. *Journal of Neurochemistry*, *161*, 463–477. https://doi.org/10.1111/jnc.15617